Soft Matter

PAPER

View Article Online
View Journal | View Issue

Cite this: *Soft Matter*, 2025, **21**, 2623

Development of biobased poly(urethanes-*co*-oxazolidones) organogels†

Salvatore Impemba, ‡[bc] Damiano Bandelli, ‡[a] Rosangela Mastrangelo, [b] Giovanna Poggi, [a] David Chelazzi *[a] and Piero Baglioni *[b]

Received 8th January 2025,
Accepted 5th March 2025

DOI: 10.1039/d5sm00020c

rsc.li/soft-matter-journal

Polyurethanes are largely employed in various fields such as building, insulation and adhesive industries, but there is the constant need to develop sustainable formulations using "green" components and feasible processes. Here, a new series of sustainable castor oil and epoxidized castor oil-based (CO/EpCO) polyurethane networks was synthetized and characterized. The added epoxy functions react with isocyanates forming oxazolidinone linkages in the gels' network, reducing the gelation time from over 3 hours up to 0.5 hours, increasing thermal resistance from 385 °C to 400 °C, tuning the gels' chemical affinity to organic solvents, and modulating some of their structural features at the nanoscale (*e.g.*, polymer mesh size and characteristic persistence lengths), which altogether affect the mechanical behavior and the functionality of the gels. The key features of the new gels are fast gelation, good mechanical properties in the solvent-less and swollen states, and interactions with organic solvents, together with the high sustainability of the whole syntethic process. These features make the novel poly(urethanes-*co*-oxazolidones) castor oil organogels promising sustainable materials for potential use in several scientific and technological fields, ranging from cleaning/detergency to the adhesives and sealant industry.

Introduction

Since their introduction in the early 20th century, and following the postwar boom, polymers have become ubiquitous in scientific and technological applications.[1] Recently, however, growing issues and concerns related to the production, use, and disposal of classic polymeric materials from oil sources, have pushed research towards more sustainable alternatives. Vegetable oils from renewable sources are of high interest since they are cost competitive and can be used to produce sustainable biofuels and industrial raw materials, replacing fossil feedstock.[2] Accordingly, polymeric materials produced from renewable sources have gained growing attention in various fields, spanning from paints to cosmetics, coatings, and lubricants.[3–6] Some examples include polyurethane, polyesteramide, and polyetheramide produced from natural oils, which are considered biodegradable, non-toxic, and easy to modify, in addition to the large availability of their monomers, and are thus used for different applications in several sectors.[7–9] In particular, polyurethanes are versatile polymers that can be largely employed in coatings, adhesives, and textile sizing.[10] As a result, vegetable oil-based polyols are gaining importance as alternatives to hydrocarbon-based feedstocks for the synthesis of this class of polymers.[11] Among natural oil polyols, castor oil (CO) is the only commercially available material directly produced by nature, and can be used to synthesize coatings, elastomers, foams, sealants and adhesives.[11] The castor bean plant, *Ricinus communis*, is grown worldwide and its seed oil has been applied in many materials.[12–18] CO is produced with high yields, and is a sustainable, renewable source that does not impact on the food chain (being nonedible).[11,19] Research in CO-based polyurethanes is far from concluded, with virtually unlimited perspectives, but poses significant challenges to devise time- and cost-effective processes and highly performing materials.[10,20]

Targeting these issues, we propose in this work a new class of bio-based organogels obtained from CO and epoxidized castor oil (EpCO).

Recently, we demonstrated the employment of CO to synthesize polyurethane gel networks with promising properties as sustainable and biodegradable pollutant adsorbers or cleaning tools.[21–25] These systems constitute an advantageous class of organogels owing to their feasible and low-energy preparation routes, the use of a renewable source (CO) to build the gel network, and the formation of the network without using

[a] *Department of Chemistry "Ugo Schiff", University of Florence, via della Lastruccia 3, Sesto Fiorentino, Florence, Italy. E-mail: david.chelazzi@unifi.it*
[b] *Department of Chemistry "Ugo Schiff" and CSGI, University of Florence, via della Lastruccia 3, Sesto Fiorentino, Florence, Italy. E-mail: baglioni@csgi.unifi.it*
[c] *Department of Chemistry and Biology, University of Salerno, Fisciano, Salerno I-84084, Italy*

† Electronic supplementary information (ESI) available. See DOI: https://doi.org/10.1039/d5sm00020c

‡ These authors contributed equally.

solvents or purification steps, differently from other examples of organogels reported in the literature.[26–32] However, despite the promising studies carried out so far, there is large room to devise new systems capable of adapting to different tasks, by modifying the CO chains to obtain specific structural, dynamic and functional properties.

In particular, CO can be used to modify epoxy resins and obtain materials for special uses.[33–42] Moreover, the presence of carbon–carbon double bonds makes the CO molecule particularly suitable for epoxidation. To this aim, different catalytic systems, based on biological, organic and inorganic pathways, can be used in the epoxidation process.[43–45]

Several polymeric nanocomposites can be prepared from EpCO and montmorillonite clay with efficient mechanical properties compared with traditional polymers.[46] Furthermore, EpCO represents an interesting bio-based building block for the chemical industry to produce fatty acid carbonates,[47,48] which in turn have a variety of applications.[49–52]

The use of epoxidized reactants can alter the physico-chemical properties of the resulting rubbers due to its functionalization with oxirane moieties. For instance, the use of epoxidized reactants in the presence of isocyanates can lead to the formation of oxazolidinone linkages capable of varying crosslinking density (Scheme 1). Moreover, the presence of epoxide moieties in the final material can be beneficial to tune features such as solvent entrapment and (bio)degradability.[53,54]

In this work a new series of CO/EpCO-based polyurethane/oxazolidinones networks was synthetized and characterized. Prior to the study of the cured EpCO/CO samples, a preliminary study of EpCO was performed by means of both proton nuclear magnetic resonance (^{1}H NMR) and size exclusion chromatography (SEC). Subsequently, the estimation of gelation times was performed *via* rheological analysis for a series of selected samples. The final CO/EpCO gels were characterized by RAMAN and 2D-FTIR spectroscopy, thermogravimetric analysis (TGA), and by Small angle X-ray scattering (SAXS) to access their structural features at the micro- and nano-scale and to verify the presence of oxazolidinone linkages. Rheological measurements were carried out to characterize the mechanical behavior of the final materials. The main rationale was to devise a new sustainable platform of polyurethane-based systems with enhanced performances of interest in transversal scientific and technological fields, since epoxy castor oil and its derivates are applied in several sectors.[55–59] In the field of coatings and adhesives for example, the partial replacement of CO with EpCO in a specific material, could be beneficial to improve adhesion to specific surfaces.[60,61]

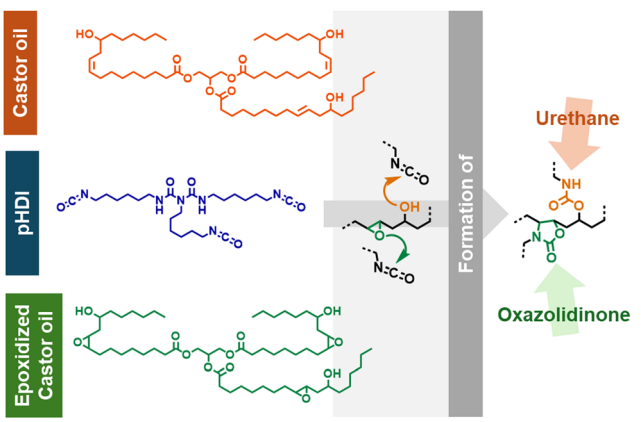

Scheme 1 Representation of the reaction between CO, EpCO and pHDI (poly(hexamethylene diisocyanate)).

Materials and methods

Materials

Castor oil (CO, viscosity: 2.11×10^{-4} m^2 s^{-1} at 40 °C, Guinama), epoxy Castor oil (EpCO, Specific Polymers) and poly (hexamethylene diisocyanate) (pHDI, viscosity: 1.3–2.2 PA s at 25 °C, Sigma-Aldrich) were used as received for the preparation of the gels, without any purification. Diethyl carbonate (DEC, 99–100%, Carlo Erba), ethyl methyl ketone (MEK, 99.5%, Carlo Erba) and acetone (99.5%, Sigma-Aldrich) were used as received.

Preparation of organogels

Five series of CO/EpCO-based organogel gums were prepared using pHDI as crosslinker. The composition of these systems, obtained by changing the ratio between CO and EpCO, and keeping the quantity of pHDI fixed (18% wt compared to CO + EpCO), is reported in Table 1. For comparison, a gel with only CO was also prepared, as a reference system.

The gels were all prepared following the same synthetic procedure, regardless of the initial mix composition: CO, EpCO, and pHDI were placed in a vial of 40 mL at room temperature. The reaction mixture was heated at 60 °C and stirred for 30 min to obtain a pre-polymer viscous liquid. Then, the pre-polymer solution was poured in 10×14 cm^2 molds, to obtain sheets with a thickness of 2 mm. The molds were cured at 60 °C in an oven for 16 h. The final systems were then removed from the molds and employed for further characterization.

Swelling degree of organogels

When immersed in organic solvents, the cured gels increase in size and weight. The amount of solvent adsorbed by the polymeric network was measured gravimetrically at different loading times to calculate the swelling degree (S):

$$S(\%) = (W_s - W_d)/W_d \times 100$$

where W_s is the weight of the swollen gel at a particular time and W_d is the weight of the corresponding dry system. Measurements were repeated at least three times.

Table 1 Name and composition of the five systems

Code	CO[a] (wt%)	EpCO[a] (wt%)
SD 1	100	0
SD 2	70	30
SD 3	50	50
SD 4	0	100

[a] Fraction of CO or EpCO over the total CO and EpCO content.

Instruments

Size exclusion chromatography (SEC). SEC measurements were performed utilizing a system composed of a Shodex ERC-3215α degasser connected with a Waters 1525 binary HPLC pump, a Waters 1500 series heater set at 40 °C, a Wyatt Viscostar-II detector and a Wyatt OPTILAB T-rEX detector, three Shodex columns (GPC KF-802.5, GPC KF-803 and GPC KF-804) employing THF as eluent with a flow rate of 1.0 mL min^{-1}. A set of polystyrene standards (PS, 400 g $mol^{-1} < M_p < 50$ kg mol^{-1}) samples were purchased from shodex and used for calibration. All data evaluation was performed according to standard procedures employing ASTRA software.

Nuclear magnetic resonance (NMR). NMR were measured at 25 °C on a Bruker AVIII400 UltraShield Plus spectrometer in deuterated THF (THF-d_8). The residual ^{1}H peak of the deuterated solvent was used for chemical shift referencing. All NMR data interpretation was performed with TopSpin software (v.3.6.4).

Rheological characterization

Rheological measurements were carried out with a TA Instrument Hybrid Rheometer DISCOVERY HR-3, using a plate-plate geometry (flat plate 20 mm diameter) and a Peltier temperature controller. The cell was closed by lowering the head to the measuring position in the axial force-controlled mode. The measurements were performed both for the pre-polymer solutions, for the dried gums and for solvent-loaded gels. Each sample was loaded onto the plate, and care was taken to minimize the stress to the sample during the loading procedure.

Oscillation time sweeps were acquired on pre-polymer solutions after 5′ since the start of the reaction, using a flat 40 mm plate with a gap of 500 μm between plates. To measure the viscoelastic properties of the material upon curing, the Peltier temperature control was set at 60 °C. Measurements were conducted at 1 Hz and 1% oscillation strain, with a sampling interval of 150 s.

On cured systems, measurements were performed at 25 °C, with no soak time and repeated at least three times. Amplitude sweep tests (c = 0.01–10%; 1 Hz) were performed to determine the linear viscoelastic (LVE) region. Frequency sweep measurements were then carried out over the frequency range 0.01–10 Hz at a constant strain within LVE region.

Thermal gravimetric analysis (TGA)

The thermal behaviour of gels was studied by TGA using an SDT Q600 TA Instrument, operating between 30 and 500 °C at a heating rate of 10 °C min^{-1} under nitrogen flow (100 mL min^{-1}). Measurements were repeated at last three times. For each measurement, about 10 mg of sample was placed inside an alumina pan and analysed.

Differential scanning calorimetry (DSC)

DSC measurements were carried out with a Discovery DSC2500 (TA Instruments) apparatus. Scans from −90 °C to 25 °C at a heating rate of 10 °C min^{-1} were acquired on samples loaded in sealed Tzero aluminum pans.

Raman spectroscopy analysis

Raman spectra were acquired in different areas of the gel samples with an in *Via* Qontor confocal microRaman by Renishaw. The instrument is equipped with a 532 nm laser (200 mW, 1800 L mm^{-1} grating) and a front-illuminated CCD camera. Representative spectra are reported.

Fourier-transform infrared (FTIR) spectroscopy imaging

The 2D FTIR imaging of the gels was carried out using a Cary 620–670 FTIR microscope equipped with a Focal Plane Array (FPA) 128 × 128 detector (Agilent Technologies). This set-up was selected as it allows discriminating compounds with different chemical composition on a surface down to a spatial resolution of few microns.[62] The spectra were recorded directly on the surface of the organogels (or of the Au background) in reflectance mode, using an open aperture, a spectral resolution of 8 cm^{-1}, and acquiring 128 scans for each pixel. The ''single-tile'' analysis yields a false-colour IR map of *ca.* 700 × 700 μm^2, with each pixel providing an independent spectrum over an area of 5.5 × 5.5 μm^2. The chromatic scale depends on the intensity of the imaged IR absorption in each map, ranging from high intensity (red pixels) to low or no intensity (azure or blue pixels).

Small-angle X-ray scattering (SAXS) measurements

SAXS measurements were performed using a HECUS S3-Micro (Kratky-type camera) equipped with a position-sensitive detector (OED 50M) featuring 1024 channels of 54 μm. Cu Kα radiation of wavelength λ = 1.542 Å was provide by a GeniX X-ray generator (Xenocs, Grenoble) working with a microfocus sealed-tube (power: 50 W). The volume between the sample and the detector was kept under vacuum during the measurements to minimize air scattering. SAXS curves were obtained in the Q-range between 0.0045 and 0.3 $Å^{-1}$. Gel samples were placed into a 1 mm-thick cell for solid samples, with Kapton film as window. Measurements were performed at 25 °C. Scattering curves were corrected for the empty cell contribution, considering the scattering of the Kapton film windows and the relative transmission factors.

Results and discussion

The aim of the present work is the development of novel polyurethane organogels based on castor oil and epoxidized castor oil. To this aim, a commercially available epoxidized castor oil (EpCO), with 2.92 and 2.42 meq g^{-1} of epoxide content and hydroxyl groups, respectively, was employed for synthesis. Prior to its use as a reactant, the epoxidized castor oil was analysed by means of size exclusion chromatography (SEC) in THF eluent to gain insights on its molar mass employing a system equipped with viscometer and refractive index detectors. As a result, three main distributions were detected from both

detectors, indicating the presence of oligomeric species. To access the estimation of molar masses according to universal calibration, the mass of each species was estimated employing eqn (1):

$$A_{i,\mathrm{RI}} = K_{\mathrm{RI}} \times m_i \times \frac{\mathrm{d}n}{\mathrm{d}C} \quad (1)$$

where $A_{i,\mathrm{RI}}$ is the area of the ith peak, K_{RI} is the instrument calibration constant, m_i is the mass of sample corresponding to the ith peak, and the $\mathrm{d}n/\mathrm{d}C$ is the refractive index increment of the ith species that was hypothesized to be constant for all the peaks.

The results indicated that the most abundant species (81.6 m% of the sample) featured a number average molar mass (M_n) of 948 g mol^{-1} and a low dispersity value ($Đ$) of 1.11, in line with a monomeric epoxidized castor oil (Fig. 1). The two additional species corresponded to a M_n of 2170 g mol^{-1} (10.5 m%, $Đ$ = 1.10) and 4659 g mol^{-1} (7.90 m%, $Đ$ = 1.06), suggesting the presence of oligomeric species (dimeric and tetrameric, respectively).

In addition to SEC analysis, proton nuclear magnetic analyses were performed on EpCO to assess the presence of unsaturated hydrogens. The comparison between EpCO and CO spectra revealed the absence of signals corresponding to unsaturated bonds at 5.40 ppm for EpCO, in line with a full conversion to epoxide groups and were furthermore confirmed from HSQC-NMR and HMBC-NMR analysis (Fig. S1, ESI†). The effect of epoxidation also resulted in the absence of signals between 1.95 and 2.20 ppm ascribed to allylic protons, while resulted in new signals in the regions between 2.70 and 3.10 ppm related to hydrogens bound with the peroxide's carbon atoms.

Following this preliminary insight on the EpCO structure, castor oil and epoxided castor oil were mixed at a target mass ratio of 100 : 0 (SD 1), 70 : 30 (SD 2), 50 : 50 (SD 3) or 0 : 100 (SD 4) (Table 1). The mixture was heated at 60 °C and pHDI (polyhexamethylene diisocyanate) was added to the CO/EpCO mixture to achieve a pHDI to CO/EpCO ratio of 18% to 82 m% in line with previous publications.[1,21,22,25] In particular, the use of such reactants feed allows to obtain COPU products stable to mechanical friction and toward swelling in selected solvents, that is a central step for developing and studying new materials with applications for gel, rubbers and sealants.

Gelation times were obtained through time sweep analysis of the pre-gel crude reaction mixtures at 60 °C (Fig. 2). A gelation time of ~3.2 hours was obtained from SD 1 gels containing CO and pHDI (82 and 18 m%, respectively), as previously reported.[21] In contrast, the use of EpCO resulted in faster gelation times up to 0.5 h for SD 4 (where CO is fully replaced with EpCO), showing a SD 1 > SD 2 > SD 3 > SD 4 trend.

Fast gelation times are typically desired, *e.g.* to reduce the curing time of adhesives, making the addition of EpCO in the reaction mixture pivotal for the fast, controlled formation of three-dimensional crosslinked CO-based structures. In principle, differences in gelation time can be ascribed to different capability of forming the three-dimensional gel network.

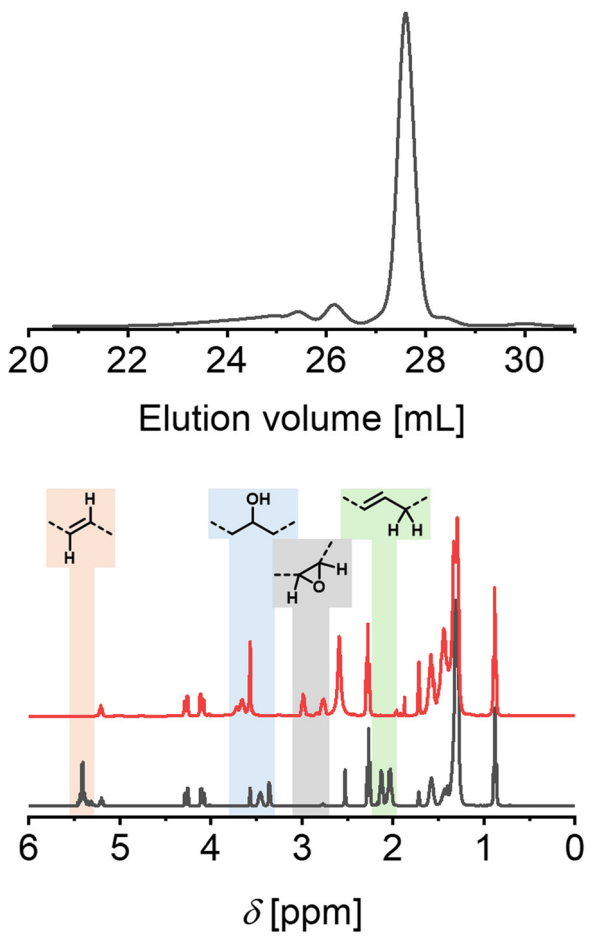

Fig. 1 Analysis of EpCO. Top: SEC curves (refractive index detector). Bottom: Overlay of proton nuclear magnetic spectra of CO (black) and EpCO (red), and assignments of peaks related to epoxidation.

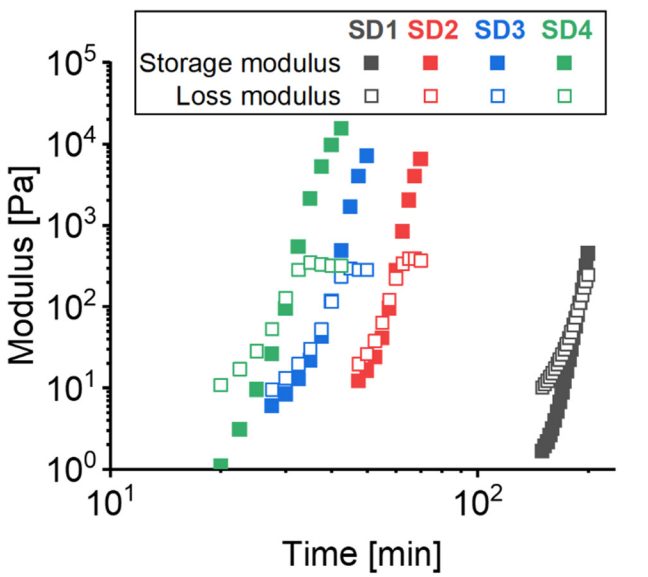

Fig. 2 Time sweep rheological analysis of the pre-gel mixtures SD 1 to SD 4.

Recently, we have demonstrated that oligomeric additives with well-defined hydrophobicity can act as compatibilizers to tune gelation times in CO-based polyurethane networks.[1,21] Given the similar structure of CO and EpCO, in this case the gelation time variation is likely due to the known capacity of epoxides to react with isocyanates resulting in the formation of oxazolidinone linkages in a fast and controlled manner.[63–65] The formation of such linkages can occur along with the formation of urethane bonds, *i.e.* obtained by the reaction of hydroxyl groups with isocyanate, resulting in a gelation speed-up (see Scheme 1).

Additional information on the presence of oxazolidinone species were obtained by RAMAN analysis of the cured gels after 16 hours reaction (Fig. 3). The typical peak of the isocyanate ═(–NCO) at *ca.* 2270 cm^{-1} is absent in all the gelled samples. In contrast, the CO and EpCO containing gels SD 1 to SD 4 showed similar peaks at 1545 and 1280 cm^{-1} assigned to the vibration in the carbamate bond (R–NH═CO), confirming the excellent conversion of isocyanate to urethane bonds. Other characteristic peaks fall at 1759 cm^{-1} (–C═O stretching of the triglyceride ester carbonyls), 2950 and 2860 cm^{-1} (asymmetric and symmetric vibrations of aliphatic $–CH_2$ fatty acid hydrocarbon chains), 1473 cm^{-1} (bending of $–CH_2$ aliphatic group), and 1280, 1187, 1100 and 1074 cm^{-1} (bending vibrations of ester carbonyl groups). Interestingly, all the CO-containing gels show a peak at 1655 cm^{-1} related to C═C stretching. A peak at 1637 cm^{-1} can be seen for the ECO-based gel SD 4, which cannot be related to C═C due to the full epoxidation of the sample. Such absorption is typically found in the spectra of oxazolidones and can be, therefore, connected with the formation of these new linkages.[63] However, gels SD 2 and SD 3, obtained with a mixture of EpCO and CO showed a broad peak containing both oxazolidone and C═C stretching contributions (Fig. 3, left).

To decouple oxazolidinone and C═C contributions between 1580 and 1700 cm^{-1}, the spectra obtained from SD 1 to SD 3 were deconvoluted using two Gaussian contributions fixed at 1640 and 1656 cm^{-1}. The ratio of the areas underlying the curves was calculated according to eqn (2).

$$X = \frac{A_{1656}}{A_{1640}} \times M_{f,CO} \quad (2)$$

where $M_{f,CO}$ is the mass fraction of CO in the sample.

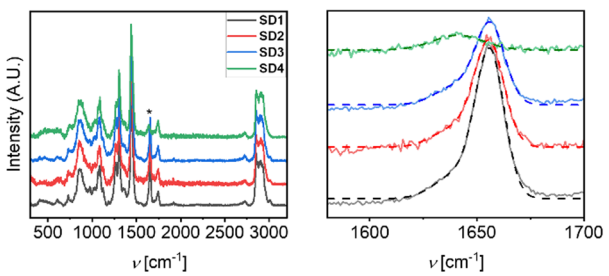

Fig. 3 RAMAN analysis of the cured SD 1 to SD 4 gels. Left: Traces overlay. Right zoom in in the region between 1580 and 1700 cm^{-1} of the RAMAN curves (full lines) related to both C═C and oxazolidone stretching frequencies and fitting according to Gaussian extrapolation (peaks at 1640 and 1656 cm^{-1}, dotted lines).

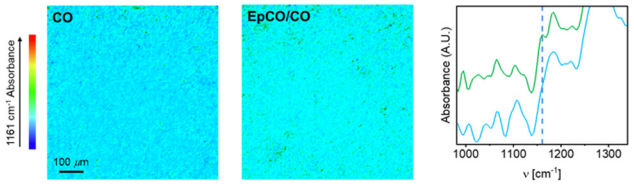

Fig. 4 2D FTIR imaging of the 1161 cm^{-1} peak (–C–O stretching) in the spectra of CO and EpCO/CO gels. Green pixels indicate regions of the gels' surface where the peak is observed in addition to the CO polyurethane absorptions (pixel size is 5.5 × 5.5 μm^2). Blue-azure pixels indicate regions where the peak was not observed. Representative IR Reflectance spectra are included in the bottom-right panel, related to green pixels (green line) or blue-azure pixels (blue line).

As expected, maximum X value was found for SD 1 (0.25), decreasing as EpCO ia added with the trend SD 1 > SD 2 (0.21) > SD 3 (0.17) > SD 4 (0). It follows that the decrease of X values corresponds to an increase of new oxazolidone linkages, supporting the initial hypothesis.

Consistently with RAMAN data, FTIR 2D imaging highlighted, in the EpCO- containing gels, the presence of a peak at 1161 cm^{-1} (green pixels on azure background in Fig. 4) in addition to the CO polyurethane absorptions, ascribable to ether or ester C–O stretching bonds in unreacted epoxy groups or oxazolidone species.

As a result, FTIR 2D analysis revealed the presence of regions of tens of microns ascribed to epoxy-containing regions (green pixels in Fig. 4) that are phase separated to the pHDI and CO regions.

Overall, the use of epoxidized castor oil for the new castor oil organogels enabled the formation of oxazolidone crosslinks, in addition to the urethane bonds, which are expected to affect the gels' properties due to the variation of crosslinking density.

Indeed, different degradation patterns were measured by TGA on the four formulations (Fig. 5). Briefly, a first main thermal event is located between 270 and 410 °C, which can be ascribed to the degradation of urethane linkage and/or volatilization of highly volatile and unstable compounds such as oxygenated compounds, hydroperoxides, and polyunsaturated fatty acids. Two additional steps were observed in the range 410–450 °C and 450–490 °C, which correspond to the decomposition of monosaturated and saturated fatty acids, respectively.

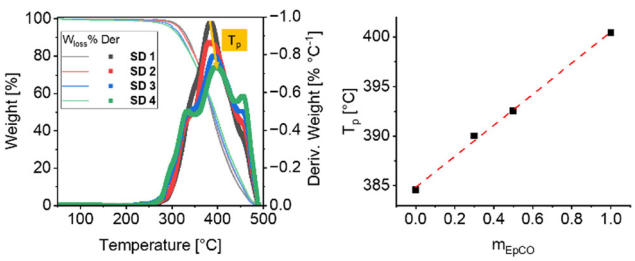

Fig. 5 TGA analysis of the SD 1 to SD 4 samples. Left: Weight loss (line) and derivative weight loss curves (dots) and depiction of the derivative peak temperature (T_p) of the more intense degradation step. Right: Evolution of T_p over mass fraction of EpCO over CO; the dotted line is a guide.

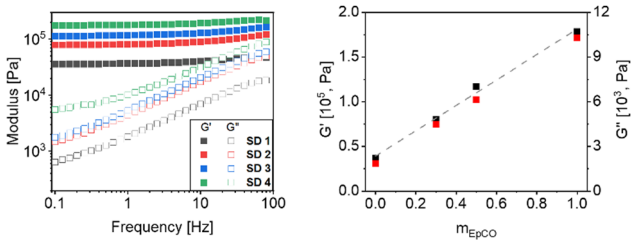

Fig. 6 Rheological analysis of samples SD 1 to SD 4. Left: Frequency sweep curves of gels. Right: Plot of G' and G'' at 1 Hz *vs.* mass fraction of EpCO over CO; the dotted line is a guide.

Interestingly, the evolution of the most intense derivative peak temperature (T_p), corresponding to the peak obtained in the 380–410 °C region, featured a linear increase with the mass fraction of EpCO over CO (m_{EpCO}) suggesting that the presence of oxazolidinone bonds can alter the overall thermal properties of the final gels (Fig. 5).[66]

The rheological behaviour of all the investigated systems (see Fig. 6) is typical of a viscoelastic solid, as advisable for a gel, rubber or a cured sealant/adhesive. Frequency sweeps revealed that the addition of EpCO in the mixture CO/pHDI resulted in higher storage modulus (G'), up to 180 kPa for SD 4. The loss modulus (G'') showed the same increase (Fig. 6). In line with thermal data, also G' and G'' featured a linear increase over m_{EpCO} revealing the possibility to tune mechanical properties by varying the EpCO content in the formulation.

Additional information on the SD gels were accessed by means of glass transition temperature (T_g) evaluation obtained by means of differential scanning calorimetry (DSC) analysis.

The T_g of these systems, confirms the effect of the isocyanate content on the mechanical properties of the material. Indeed, SD 1, which only contains CO and pHDI, has a T_g of −47.1 °C, while SD 4 displays a T_g of −26.1 °C. Indeed, the T_g increased linearly with the content of EpCO in the EpCO/CO mixture.

These values are in line with those of polyurethane networks reported in the literature,[67] and clearly indicate that the gels will be in rubbery state when applied at room temperature, where chain mobility can facilitate mechanical compliance and thus favour the adaptability of the PU to curved surfaces.

Gels' inhomogeneities at the nanoscale were investigated through SAXS measurements. SAXS curves fitting was performed according to a Porod-Guinier model, based on the literature[68–70] and our previous observation on similar systems (eqn (3)):[22]

$$I(Q) = \frac{I_P}{Q^n} + I_G \cdot e^{-\frac{1}{3}(R_G Q)^2 \infty} + Bkg \qquad (3)$$

where I_P and I_G are the scales of Porod and Guinier terms, respectively, n is the Porod slope, R_G is the gyration radius of networks inhomogeneities (indicating dense, crosslinked areas), and *Bkg* the background.

SAXS data analysis (Fig. 7) showed that the inclusion of EpCO in the crosslinked CO matrices, leads to the formation of inhomogeneities of about 4 nm (R_G values of SD 2–SD 3 in Table 2). No inhomogeneities in the nanometers range

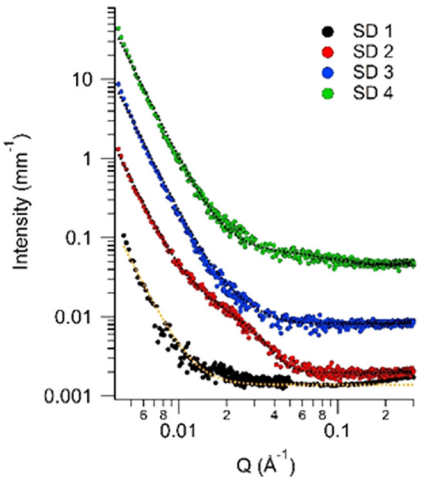

Fig. 7 SAXS data (markers) and fitting curves (dotted lines) of the SD 1 to SD 4 systems. Curves have been shifted along the y-axis for clarity.

Table 2 Fitting parameters obtained by fitting SAXS data of the CO/EpCO gels

Sample	I_n ($\times 10^{-10}$)	n	I_G ($\times 10^{-2}$)	R_G (Å)
SD 1	1.7 ± 0.1	4.00 ± 0.05	—	—
SD 2	7.4 ± 0.1	4.00 ± 0.05	5.4 ± 0.2	39 ± 1
SD 3	20.5 ± 0.1	4.00 ± 0.05	1.0 ± 0.2	39 ± 1
SD 4	18.2 ± 0.1	4.00 ± 0.05	0.5 ± 0.2	12 ± 1

emerged in the pure CO sample (SD 1), while the SD 4 formed with only EpCO and pHDI, showed few inhomogeneities of about 1 nm. The porod slope at low-Q indicates the presence of larger inhomogeneities (>1 μm, *i.e.* not detectable in the investigated Q-range) with a smooth surface, likely linked to an initial CO-pHDI incompatibility during mixing, observed in laboratory tests.

The detection of nanoscale inhomogeneities with different sizes is likely related to the formation of different types of crosslinks as the CO-EpCO ratio varies, in agreement with the gelation points experiments and TGA results. In other words, crosslinks might be mixed and more polydisperse in bicomponent systems, due to the higher reactivity of EpCO toward pHDI.

Considering the latter, it is plausible that crosslinked regions in SD 4 will be more ramified than in SD 1 network, resulting in larger R_G inhomogeneities. We cannot exclude, however, that the lack of inhomogeneities in SD 1 might be the result of lower contrast in this system (Fig. 7).

Overall, we can conclude that the use of EpCO allows to tune mechanical properties and crosslinking density in the matrices.

The use of additives in polyurethanes can also lead to different interactions with solvents, with applications in several fields, such as the cleaning of works of art, where the castor oil gels are used as sponges to remove aged varnishes, the purification of waste waters, where the gels can be used to selectively uptake solvents contaminating water, or in the sealant industries, where solvents can be used to ease the removal of cured polyurethane adhesives.

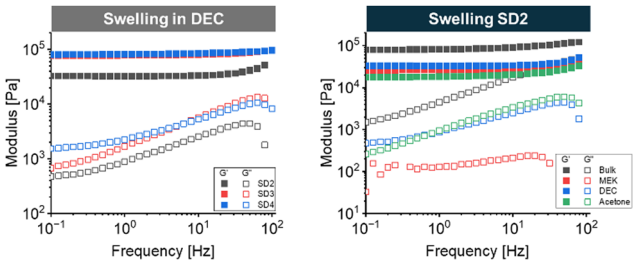

Fig. 8 Amplitude sweep experiments of EpCO-CO based gels. Left. Rheology of SD 2 to SD 4 after swelling in DEC for 0.5 h. Right. Rheology of SD 2 after swelling for 0.5 h in MEK, DEC, and acetone and FS of the initial material (bulk).

The newly developed CO/EpCO gels were swollen in some "green" organic solvents, *i.e.*, acetone, methyl ethyl ketone (MEK) and diethyl carbonate (DEC), for 30 minutes. In all cases, the swelling degree followed the trend SD 1 > SD 4 > SD 3 > SD 2 (Table S1, ESI†). In principle, the behaviour of SD 1 could be related to its lower crosslinking density, that could be beneficial for solvent entrapment, since the increase of ramifications in the three-dimensional gel's structure impairs solvophobic features. However, the addition of EpCO can result in the presence of unreacted epoxide rings in the three-dimensional gel structure as outlined from IR data. It is likely the balance of crosslinking density, type of crosslinking bonds (urethane *vs.* oxazolidones), and presence of unreacted polar groups, which overall concur to determine the swelling degree.

Frequency Sweeps performed on CO/EpCO systems in DEC after 0.5 h swelling time (Fig. 8-left) showed that the swollen SD 2 gel has the lowest storage and loss moduli, ~32 and 0.9 kPa (at 1 Hz), while SD 3 and SD 4 featured a G' of ~80 kPa and a G'' of ~2 kPa (at 1 Hz), *i.e.*, addition of EpCO beyond 30% yields higher crosslinking density and a lower decrease of mechanical properties upon swelling. The replacement of DEC with MEK and acetone resulted in further decrease of G', suggesting that these organic solvents could be feasibly used for the swelling and the removal of adhesives or sealants based on the new CO/EpCO formulations, a possible important application of these new gels adding to current castor oil adhesives.[71]

In summary, we demonstrated how new "green", sustainable poly(urethanes-*co*-oxazolidones) organogels can be formulated and modulated by addition of EpCO to tailor their structure, thermal and rheological behaviour, and swelling in organic solvents, elucidating the effect of EpCO addition on some important physico-chemical properties, with potential application in several of applicative fields.

Conclusions

A series of new "green", sustainable poly(urethanes-*co*-oxazolidones) organogels, based on castor oil and its epoxidized derivative (EpCO), was prepared and characterized, with potential applications in the polyurethane chemistry research and industry. The effect of EpCO addition on some important physico-chemical properties was elucidated. During gel curing, the use of EpCO enabled to increase the speed of the polyurethane network formation, likely due to the capability of epoxides to react with isocyanates forming oxazolidinone linkages. RAMAN and FTIR microscopy confirmed the presence of these functionalities in the cured gels. The presence of oxazolidinone linkages determined the variation of relevant physico-chemical properties in a controlled manner in the gels, by simply varying the initial EpCO-CO reaction feed. Namely, the thermal and rheological behaviour, the nanoscale structure (studied through SAXS), and the swelling behaviour of the gels in some "green" organic solvents, were controlled by EpCO addition. Overall, the present work enabled the development of a new class of organogels with fast gelation, good mechanical properties in the solvent-less and swollen states, and interactions with solvents, together with high sustainability of the whole synthetic process.

In principle, the combined variations of reaction features, nanostructures, mechanical and thermal properties can be obtained by varying reactants feed, or by employing additives.[1,22] The variation of isocyanate feed can be beneficial to act on the abovementioned properties. For instance, the increase of material's stiffness can be accessed by increasing crosslinker agent. In contrast, the use of sustainable additives can be beneficial to obtain materials with higher stiffness but also affect the formation of micrometric domains. For this reason, the use of sustainable epoxidized reactants can be of outmost interest to access new materials with unperturbed microstructure, enabling the decoupling of such features, and avoiding the increase of isocyanate feed, and therefore reducing the amount of highly reactive species. These properties make the new organogels potential candidates for use as sponges, rubbers, adhesives and sealants in different applications, simply playing on the reactants feeds. Being based on the highly sustainable castor oil and its epoxidized counterpart, the new gels represent thus promising materials for different industrial sectors, while also complying with sustainability and zero-impact socio-economical challenges.

Author contributions

Salvatore Impemba: conceptualization, methodology, formal analysis, investigation, data curation, writing – original draft. Damiano Bandelli: conceptualization, methodology, visualization, writing – original draft, writing – review & editing. Rosangela Mastrangelo: formal analysis, investigation, data curation, writing – original draft, writing – review & editing. Giovanna Poggi: data curation, methodology, writing – review & editing, supervision, funding acquisition. David Chelazzi: validation, methodology, writing – review & editing, supervision, funding acquisition. Piero Baglioni: validation, resources, writing – review & editing, supervision, funding acquisition.

Data availability

The data supporting this article have been included in the main text or as part of the ESI.† Raw data are available upon request to the authors.

Conflicts of interest

There are no conflicts to declare.

Acknowledgements

CSGI and the European Union (GREENART project, Horizon Europe research and innovation program under grant agreement no. 101060941) are gratefully acknowledged for financial support. Views and opinions expressed are however those of the author(s) only and do not necessarily reflect those of the European Union or the European Research Executive Agency (REA). Neither the European Union nor the granting authority can be held responsible for them. DC and DB acknowledge the Project PE 0000020 CHANGES – CUP [SPOKE 7, WP5], NRP Mission 4 Component 2 Investment 1.3, Funded by the European Union – NextGenerationEU for financial support. The publication was made by a researcher (DB) with a research contract funded by the European Union-PNRR NextGeneration-EU in accordance with Article 24, paragraph 3a of Law No. 240 of December 30, 2010, as amended and Ministerial Decree No. 1365 of November 8, 2022 and by a researcher (RM) with a research contract co-funded by the European Union – PON Research and Innovation 2014–2020 in accordance with Article 24, paragraph 3a of Law No. 240 of December 30, 2010, as amended and Ministerial Decree No. 1062 of August 10, 2021.

References

1 D. Bandelli, R. Mastrangelo, G. Poggi, D. Chelazzi and P. Baglioni, New sustainable polymers and oligomers for Cultural Heritage conservation, *Chem. Sci.*, 2024, **15**, 2443–2455.
2 J. M. Dyer, S. Stymne, A. G. Green and A. S. Carlsson, High-value oils from plants, *Plant J.*, 2008, **54**, 640–655.
3 N. Aiman Syafiq Mohd Hamidi, W. Mohamad Ikhmal Wan Mohamad Kamaruzzaman, N. Amirah Mohd Nasir, M. Syaizwadi Shaifudin and M. Sabri Mohd Ghazali, Potential Application of Plant-Based Derivatives as Green Components in Functional Coatings: A Review, *Cleaner Mater.*, 2022, **4**, 100097.
4 F. Mellou, A. Varvaresou and S. Papageorgiou, Renewable sources: applications in personal care formulations, *Int. J. Cosmet. Sci.*, 2019, **41**, 517–525.
5 R. Rocca, F. Acerbi, L. Fumagalli and M. Taisch, Sustainability paradigm in the cosmetics industry: State of the art, *Clean. Waste Syst.*, 2022, **3**, 100057.
6 S. Soni and M. Agarwal, Lubricants from renewable energy sources – a review, *Green Chem. Lett. Rev.*, 2014, **7**, 359–382.
7 A. Suhane, A. Rehman and H. Khaira, Potential of non edible vegetable oils as an alternative lubricants in automotive applications, *Int. J. Eng. Res.*, 2012, **2**, 1330.
8 J. T. P. Derksen, F. Petrus Cuperus and P. Kolster, Renewable resources in coatings technology: a review, *Prog. Org. Coat.*, 1996, **27**, 45–53.
9 S. I. Bhat, M. Mobin, S. Islam, S. Zehra and I. Shahid Ul, Recent advances in anticorrosive coatings based on sustainable polymers: Challenges and perspectives, *Surf. Coat. Technol.*, 2024, **480**, 130596.
10 A. Shirke, B. Dholakiya and K. Kuperkar, Novel applications of castor oil based polyurethanes: a short review, *Polym. Sci., Ser. B*, 2015, **57**, 292–297.
11 H. Mutlu and M. A. R. Meier, Castor oil as a renewable resource for the chemical industry, *Eur. J. Lipid Sci. Technol.*, 2010, **112**, 10–30.
12 D. S. Ogunniyi, Castor oil: A vital industrial raw material, *Bioresour. Technol.*, 2006, **97**, 1086–1091.
13 S. Kim and H. Chung, Fully biomass-based biodegradable polymers from lignin and raw castor oil: lignin-*graft*-castor oil, *Polym. Chem.*, 2023, **14**, 4126–4137.
14 M. Piccini, D. J. Leak, C. J. Chuck and A. Buchard, Polymers from sugars and unsaturated fatty acids: ADMET polymerisation of monomers derived from D-xylose, D-mannose and castor oil, *Polym. Chem.*, 2020, **11**, 2681–2691.
15 P. Furtwengler and L. Avérous, Renewable polyols for advanced polyurethane foams from diverse biomass resources, *Polym. Chem.*, 2018, **9**, 4258–4287.
16 C. Pang, J. Zhang, G. Wu, Y. Wang, H. Gao and J. Ma, Renewable polyesters derived from 10-undecenoic acid and vanillic acid with versatile properties, *Polym. Chem.*, 2014, **5**, 2843–2853.
17 A. S. More, B. Gadenne, C. Alfos and H. Cramail, AB type polyaddition route to thermoplastic polyurethanes from fatty acid derivatives, *Polym. Chem.*, 2012, **3**, 1594–1605.
18 J. M. Avramovic, A. M. Marjanović Jeromela, M. S. Krstić, B. M. Kiprovski, A. V. Veličković, D. D. Rajković and V. B. Veljković, Castor Oil Extraction: Methods and Impacts, *Sep. Purif. Rev.*, 2025, **54**, 60–82.
19 L. Pari, A. Suardi, W. Stefanoni, F. Latterini and N. Palmieri, Environmental and Economic Assessment of Castor Oil Supply Chain: A Case Study, *Sustainability*, 2020, **12**, 6339.
20 S. Maulana, E. S. Wibowo, E. Mardawati, A. H. Iswanto, A. Papadopoulos and M. A. R. Lubis, Eco-Friendly and High-Performance Bio-Polyurethane Adhesives from Vegetable Oils: A Review, *Polymers*, 2024, **16**, 1613.
21 D. Bandelli, R. Mastrangelo, G. Poggi, D. Chelazzi and P. Baglioni, Tailoring the properties of castor oil polyurethanes organogels with green oligoesters, *Colloids Surf., A*, 2024, **698**, 134528.
22 G. Poggi, H. D. Santan, J. Smets, D. Chelazzi, D. Noferini, M. L. Petruzzellis, L. Pensabene Buemi, E. Fratini and P. Baglioni, Nanostructured bio-based castor oil organogels for the cleaning of artworks, *J. Colloid Interface Sci.*, 2023, **638**, 363–374.
23 A. Zuliani, D. Chelazzi, R. Mastrangelo, R. Giorgi and P. Baglioni, Adsorption kinetics of acetic acid into ZnO/castor oil-derived polyurethanes, *J. Colloid Interface Sci.*, 2023, **632**, 74–86.
24 A. Zuliani, M. Rapisarda, D. Chelazzi, P. Baglioni and P. Rizzarelli, Synthesis, Characterization, and Soil Burial Degradation of Biobased Polyurethanes, *Polymers*, 2022, **14**, 4948.

25 A. Zuliani, D. Bandelli, D. Chelazzi, R. Giorgi and P. Baglioni, Environmentally friendly ZnO/Castor oil polyurethane composites for the gas-phase adsorption of acetic acid, *J. Colloid Interface Sci.*, 2022, **614**, 451–459.
26 P. Baglioni, N. Bonelli, D. Chelazzi, A. Chevalier, L. Dei, J. Domingues, E. Fratini, R. Giorgi and M. Martin, Organogel formulations for the cleaning of easel paintings, *Appl. Phys. A:Mater. Sci. Process.*, 2015, **121**, 857–868.
27 J. Yiming, G. Sciutto, S. Prati, E. Catelli, M. Galeotti, S. Porcinai, L. Mazzocchetti, C. Samorì, P. Galletti, L. Giorgini, E. Tagliavini and R. Mazzeo, A new bio-based organogel for the removal of wax coating from indoor bronze surfaces, *Heritage Sci.*, 2019, **7**, 34.
28 P. Ferrari, D. Chelazzi, N. Bonelli, A. Mirabile, R. Giorgi and P. Baglioni, Alkyl carbonate solvents confined in poly (ethyl methacrylate) organogels for the removal of pressure sensitive tapes (PSTs) from contemporary drawings, *J. Cult. Herit.*, 2018, **34**, 227–236.
29 T. T. Duncan, B. H. Berrie and R. G. Weiss, Soft, Peelable Organogels from Partially Hydrolyzed Poly(vinyl acetate) and Benzene-1,4-diboronic Acid: Applications to Clean Works of Art, *ACS Appl. Mater. Interfaces*, 2017, **9**, 28069–28078.
30 M. D. Pianorsi, M. Raudino, N. Bonelli, D. Chelazzi, R. Giorgi, E. Fratini and P. Baglioni, Organogels for the cleaning of artifacts, *Pure Appl. Chem.*, 2017, **89**, 3–17.
31 A. Brandolese, D. H. Lamparelli, I. Grimaldi, S. Impemba, P. Baglioni and A. W. Kleij, Access to Functionalized Polycarbonates Derived from Fatty Acid Esters via Catalytic ROCOP and Their Potential in Gel Formulations, *Macromolecules*, 2024, **57**, 3816–3823.
32 X. Zheng, X. Zhou, Y. Yang, W. Xiong, S. Ye, Y. Xu, B. Zeng, C. Yuan and L. Dai, Anchoring Solvent Molecules onto Polymer Chains Through Dynamic Interactions for a Wide Temperature Range Adaptable and Ultra-Fast Responsive Adhesive Organogels, *Adv. Funct. Mater.*, 2024, **34**, 2408351.
33 B. K. Patel, B. Patel and S. N. Desai, Novel surface coating materials based on castor oil-epoxy resin reaction products, *Chem. Sci. Trans.*, 2012, **2**, 308–314.
34 F. Zhu, Q. Fu, M. Yu, J. Zhou, N. Li and F. Wang, Synthesis and curing properties of multifunctional castor oil-based epoxy resin, *Polym. Test.*, 2023, **122**, 108017.
35 L. Zhu, F.-L. Jin and S.-J. Park, Thermal stability and fracture toughness of epoxy resins modified with epoxidized castor oil and Al_2O_3 nanoparticles, *Bull. Korean Chem. Soc.*, 2012, **33**, 2513–2516.
36 J.-L. Chen, F.-L. Jin and S.-J. Park, Thermal stability and impact and flexural properties of epoxy resins/epoxidized castor oil/nano-$CaCO_3$ ternary systems, *Macromol. Res.*, 2010, **18**, 862–867.
37 Q. Shang, J. Cheng, L. Hu, C. Bo, X. Yang, Y. Hu, C. Liu and Y. Zhou, Bio-inspired castor oil modified cellulose aerogels for oil recovery and emulsion separation, *Colloids Surf., A*, 2022, **636**, 128043.
38 M. R. Shaik, M. Alam and N. M. Alandis, Development of Castor Oil Based Poly(urethane-esteramide)/TiO2 Nanocomposites as Anticorrosive and Antimicrobial Coatings, *J. Nanomater.*, 2015, **2015**, 745217.
39 M. Derradji, X. Song, A. Q. Dayo, J. Wang and W.-B. Liu, Highly filled boron nitride-phthalonitrile nanocomposites for exigent thermally conductive applications, *Appl. Therm. Eng.*, 2017, **115**, 630–636.
40 S.-J. Park, F.-L. Jin and J.-R. Lee, Effect of Biodegradable Epoxidized Castor Oil on Physicochemical and Mechanical Properties of Epoxy Resins, *Macromol. Chem. Phys.*, 2004, **205**, 2048–2054.
41 Y. Zhang, S. Zhang, M. Zhai, B. Wei, B. Lyu and L. Liu, Self-Healing and Recyclable Castor Oil-Based Epoxy Vitrimer Based on Dual Dynamic Bonds of Disulfide and Ester Bonds, *ACS Appl. Polym. Mater.*, 2024, **6**, 8399–8408.
42 X. Liu, F. Sun, Y. Liu, B. Yao, H. Liang, M. Mu, X. Liu, H. Bi, Z. Wang, C. Qian and X. Li, Synthesis and properties of castor oil–based cationic waterborne polyurethane modified by epoxy resin, *Colloid Polym. Sci.*, 2024, **302**, 13–22.
43 H. Patil and J. Waghmare, Catalyst for epoxidation of oils: a review, *Discovery*, 2013, **3**, 10–14.
44 F. Seniha Güner, Y. Yağcı and A. Tuncer Erciyes, Polymers from triglyceride oils, *Prog. Polym. Sci.*, 2006, **31**, 633–670.
45 N. L. Parada Hernandez, A. J. Bonon, J. O. Bahú, M. I. R. Barbosa, M. R. Wolf Maciel and R. M. Filho, Epoxy monomers obtained from castor oil using a toxicity-free catalytic system, *J. Mol. Catal. A: Chem.*, 2017, **426**, 550–556.
46 S. Dhanuskar, S. N. Naik and K. K. Pant, in *Catalysis for Clean Energy and Environmental Sustainability: Biomass Conversion and Green Chemistry*, ed. K. K. Pant, S. K. Gupta and E. Ahmad, Springer International Publishing, Cham, 2021, vol. 1, pp. 209–235, DOI: **10.1007/978-3-030-65017-9_8**.
47 A. F. Guzmán, D. A. Echeverri and L. A. Rios, Carbonation of epoxidized castor oil: a new bio-based building block for the chemical industry, *J. Chem. Technol. Biotechnol.*, 2017, **92**, 1104–1110.
48 R. B. N. Prasad and B. V. S. K. Rao, in *Fatty Acids*, ed. M. U. Ahmad, AOCS Press, 2017, pp. 279–303, DOI: **10.1016/B978-0-12-809521-8.00008-8**.
49 B. Nohra, L. Candy, J.-F. Blanco, C. Guerin, Y. Raoul and Z. Mouloungui, From Petrochemical Polyurethanes to Biobased Polyhydroxyurethanes, *Macromolecules*, 2013, **46**, 3771–3792.
50 E. Rix, E. Grau, G. Chollet and H. Cramail, Synthesis of fatty acid-based non-isocyanate polyurethanes, NIPUs, in bulk and mini-emulsion, *Eur. Polym. J.*, 2016, **84**, 863–872.
51 A. Noreen, K. M. Zia, M. Zuber, S. Tabasum and A. F. Zahoor, Bio-based polyurethane: An efficient and environment friendly coating systems: A review, *Prog. Org. Coat.*, 2016, **91**, 25–32.
52 S. Devansh, P. Patil and D. V. Pinjari, Oil-based epoxy and their composites: A sustainable alternative to traditional epoxy, *J. Appl. Polym. Sci.*, 2024, **141**, e55560.
53 H. Yeganeh, M. M. Lakouraj and S. Jamshidi, Synthesis and characterization of novel biodegradable epoxy-modified polyurethane elastomers, *J. Polym. Sci., Part A: Polym. Chem.*, 2005, **43**, 2985–2996.

54 K. Ghosh, V. Kumar, D. Mishra, H. B. Patil, D. J. Kumavat, K. Ebenezer and A. R. Rao, Effect of renewable castor-oil based thermoplastic polyurethane elastomer on the thermo-mechanical and biodegradation properties of poly (lactic acid), *Mater. Today Commun.*, 2025, **43**, 111738.
55 P. Jia, M. Zhang, L. Hu, G. Feng, C. Bo and Y. Zhou, Synthesis and Application of Environmental Castor Oil Based Polyol Ester Plasticizers for Poly(vinyl chloride), *ACS Sustainable Chem. Eng.*, 2015, **3**, 2187–2193.
56 J. Chen, Z. Liu, X. Nie and J. Jiang, Synthesis and application of a novel environmental C26 diglycidyl ester plasticizer based on castor oil for poly(vinyl chloride), *J. Mater. Sci.*, 2018, **53**, 8909–8920.
57 Q. Fu, Y. Long, Y. Gao, Y. Ling, H. Qian, F. Wang and X. Zhu, Synthesis and properties of castor oil based plasticizers, *RSC Adv.*, 2019, **9**, 10049–10057.
58 W. He, H. Huang, L. Xie, C. Wang, J. Yu, S. Lu and H. Fan, The influence of self-crosslinked epoxidized castor oil on the properties of Poly (lactic acid) via dynamic vulcanization: Toughening effect, thermal properties and structures, *Colloids Surf., A*, 2021, **630**, 127517.
59 N. L. Parada Hernandez, J. O. Bahú, M. I. R. B. Schiavon, A. J. Bonon, C. I. Benites, A. L. Jardini, R. Maciel Filho and M. R. Wolf Maciel, (Epoxidized castor oil – citric acid) copolyester as a candidate polymer for biomedical applications, *J. Polym. Res.*, 2019, **26**, 149.
60 M. A. de Luca, M. Martinelli and C. C. T. Barbieri, Hybrid films synthesised from epoxidised castor oil, γ-glycidoxypropyltrimethoxysilane and tetraethoxysilane, *Prog. Org. Coat.*, 2009, **65**, 375–380.
61 M. A. de Luca, M. Martinelli, M. M. Jacobi, P. L. Becker and M. F. Ferrão, Ceramer coatings from castor oil or epoxidized castor oil and tetraethoxysilane, *J. Am. Oil Chem. Soc.*, 2006, **83**, 147–151.
62 D. Badillo-Sanchez, D. Chelazzi, R. Giorgi, A. Cincinelli and P. Baglioni, Characterization of the secondary structure of degummed Bombyx mori silk in modern and historical samples, *Polym. Degrad. Stab.*, 2018, **157**, 53–62.
63 I. Javni, A. Guo and Z. S. Petrovic, The study of oxazolidone formation from 9,10-epoxyoctadecane and phenylisocyanate, *J. Am. Oil Chem. Soc.*, 2003, **80**, 595–600.
64 J. A. Castro-Osma, A. Earlam, A. Lara-Sánchez, A. Otero and M. North, Synthesis of Oxazolidinones from Epoxides and Isocyanates Catalysed by Aluminium Heteroscorpionate Complexes, *ChemCatChem*, 2016, **8**, 2100–2108.
65 G. P. Speranza and W. J. Peppel, Preparation of Substituted 2-Oxazolidones from 1,2-Epoxides and Isocyanates, *J. Org. Chem.*, 1958, **23**, 1922–1924.
66 F. E. Golling, R. Pires, A. Hecking, J. Weikard, F. Richter, K. Danielmeier and D. Dijkstra, Polyurethanes for coatings and adhesives – chemistry and applications, *Polym. Int.*, 2019, **68**, 848–855.
67 B. Nabeth, I. Corniglion and J. P. Pascault, Influence of the composition on the glass transition temperature of polyurethane and polyurethane acrylate networks, *J. Polym. Sci., Part B: Polym. Phys.*, 1996, **34**, 401–417.
68 G. Trovati, E. A. Sanches, S. M. de Souza, A. L. dos Santos, S. C. Neto, Y. P. Mascarenhas and G. O. Chierice, Rigid and semi rigid polyurethane resins: A structural investigation using DMA, SAXS and Le Bail method, *J. Mol. Struct.*, 2014, **1075**, 589–593.
69 S. Etienne, G. Vigier, L. Cuvé and J. P. Pascault, Microstructure of segmented amorphous polyurethanes: small-angle X-ray scattering and mechanical spectroscopy studies, *Polymer*, 1994, **35**, 2737–2743.
70 R. Gallu, F. Méchin, F. Dalmas, J.-F. Gérard, R. Perrin and F. Loup, On the use of solubility parameters to investigate phase separation-morphology-mechanical behavior relationships of TPU, *Polymer*, 2020, **207**, 122882.
71 Y. Ma, X. Zhu, Y. Zhang, X. Li, X. Chang, L. Shi, S. Lv and Y. Zhang, Castor oil-based adhesives: A comprehensive review, *Ind. Crops Prod.*, 2024, **209**, 117924.

